

# Structure-based design of new poly (ADP-ribose) polymerase (PARP-1) inhibitors

Navriti Chadha<sup>1</sup> · Ameteshar Singh Jaggi<sup>2</sup> · Om Silakari<sup>1</sup> 

Received: 14 October 2016 / Accepted: 27 May 2017  
© Springer International Publishing Switzerland 2017

**Abstract** Poly (ADP-ribose) polymerase (PARP-1) is a well-established nuclear protein with prominent role in signaling and DNA repair. Various clinical candidates have been identified with the role in PARP-1 inhibition. Based on the pharmacophoric features identified from previous studies and molecular docking interactions, thiazolidine-2,4-dione derivatives have been evaluated for their PARP inhibitory activity. From an in vitro assay, 5-((1-(4-isopropylbenzyl)-1H-indol-3-yl)methylene)thiazolidine-2,4-dione (**16**) was identified as a potent inhibitor having low micromolar inhibitory activity ( $IC_{50} = 0.74 \pm 0.25 \mu\text{M}$ ). Thus, a structure-based design approach utilized in the present study helped to identify thiazolidine-2,4-dione as a novel scaffold against PARP-1 for potential development of potent anticancer therapeutics.

**Keywords** Structure-based drug design · Docking · Thiazolidine-2,4-dione · Indole · Molecular modeling · PARP

---

**Electronic supplementary material** The online version of this article (doi:10.1007/s11030-017-9754-7) contains supplementary material, which is available to authorized users.

---

✉ Om Silakari  
omsilakari@gmail.com

<sup>1</sup> Molecular Modeling Lab (MML), Department of Pharmaceutical Sciences and Drug Research, Punjabi University, Patiala 147002 Punjab, India

<sup>2</sup> Department of Pharmaceutical Sciences and Drug Research, Punjabi University, Patiala 147002, India

## Introduction

Poly (ADP-ribose) polymerase 1 (PARP-1) is the most abundant enzyme of the PARP family and is a key player for posttranslational modification of proteins in response to DNA damage and genotoxic stress [1]. The modular architecture of PARP-1 consists of three domains: (1) a DNA binding domain (DBD) or N-terminal region consisting of three zinc motifs with a role in the recognition of DNA damage and direct PARP-1 binding to damaged DNA, (2) an automodification domain (AMD) with a role in the interaction between PARP-1 and its partner proteins and (3) a catalytic domain or C-terminal region consisting of a  $\text{NAD}^+$  binding domain responsible for the catalytic function of PARP-1 [2]. Elevated levels of DNA damage stimulate PARP-1-induced poly (ADP-ribose) production, thereby exhausting the energy pools of  $\text{NAD}^+$  and ATP leading to cellular energy crisis, irreversible cytotoxicity and necrotic cell death [3]. The dramatic consequences of PARP-1 hyperactivation are frequently observed in various cancerous conditions, myocardial reperfusion injury, cardiac ischemia, stroke and diabetes-associated anomalies [4–6].

An investigation of the X-ray crystallographic structure of PARP-1 in complex with various inhibitors as well as  $\text{NAD}^+$  indicates the importance of three hydrogen bonding interactions between a carboxamide moiety and critical amino acid residues Gly202 (N–H to Gly C=O and C=O to Gly N–H) and Ser243 (C=O to Ser O–H). In addition,  $\pi - \pi$  stacking of the aromatic ring system of the inhibitor moiety with Tyr246 was found in all available crystal structures [7]. Several PARP-1 inhibitors are being investigated for their effectiveness and some are undergoing clinical investigation, including indazole-7-carboxamide (niraparib, MK-4827) [8], phthalazinone (talazoparib, BMN-673;

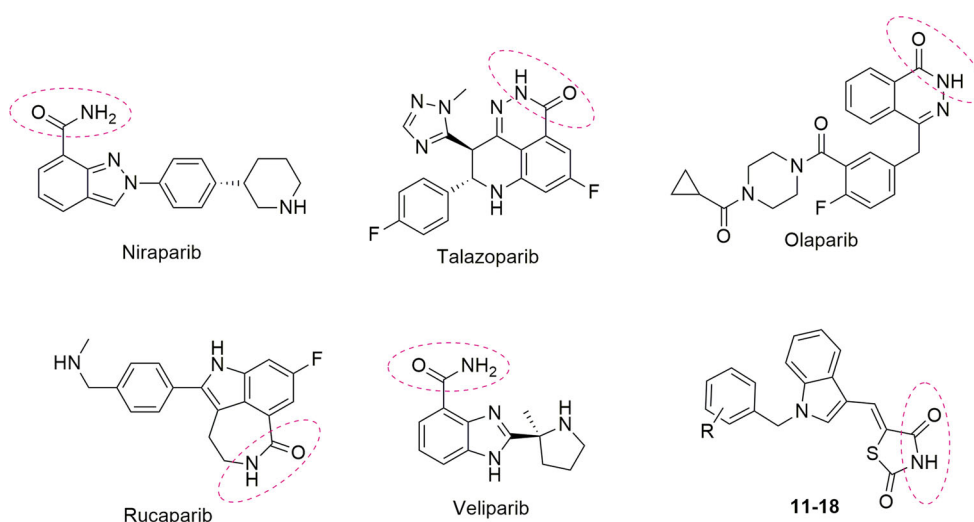


**Fig. 1** Structures of PARP-1 inhibitors under clinical evaluation

olaparib, AZD-2281) [9,10], benzimidazole-4-carboxamide (veliparib, ABT-888) [11] and azepinoindolone (rucaparib, RG014699) [12] (Fig. 1). These compounds are bicyclic or tricyclic structures with a crucial carboxamide group either rotationally constrained substituted on the ring or incorporated into the ring system to form a lactam.

Thiazolidine-2,4-dione (TZD) is a well-established heterocyclic ring system exhibiting a wide range of pharmacological activities including anti-hyperglycemic, anticancer, anti-arthritic and antimicrobial. The scaffold has shown its effectiveness against a broad spectrum of protein targets including peroxisome proliferator-activated receptor (PPAR $\gamma$ ), aldose reductase (ALR2), phosphoinositide 3-kinase (PI3K $\gamma$ ), phosphoinositide 3-kinase (PI3K $\alpha$ )/mitogen-activated protein kinase kinase (MEK), PIM kinase and protein tyrosine phosphatase 1B (PTP1B). The chemical structure of TZD and various substitutions on the scaffold provide pharmacophore guidance for targeting various protein targets [13].

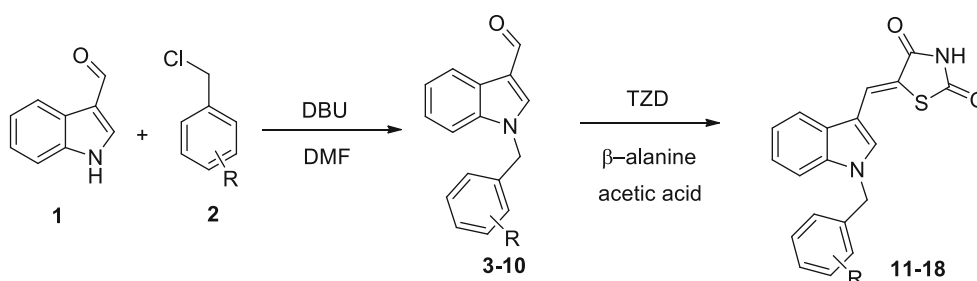
Based on the pharmacophore analysis and active site fingerprinting of PARP-1 reported in our previous studies

[14], herein we report the design, synthesis and in vitro activity of new thiazolidine-2,4-dione derivatives against PARP-1 enzyme. The TZD ring was chosen to provide the crucial for hydrogen bonding interaction with Gly202 and Ser243 of the PARP-1 active site. The TZD ring system was substituted with an indole ring to provide a ring system for  $\pi - \pi$  stacking with Tyr246. The hydrophobic pocket was observed to be fairly large; thus, the indole moiety was further substituted with different benzyl groups. The general structure of compounds **11–18** is displayed in Scheme 1.

## Results and discussion

### PARP-1 inhibitor design

An alanine scanning mutagenesis and pharmacophore analysis of PARP-1 inhibitors previously carried out by our group led to the identification of common pharmacophore required for activity characterized by the presence of a ben-



**Scheme 1** Synthesis of thiazolidine-2,4-dione analogs

Interacts with aromatic amino acids  
Tyr246 and Tyr235

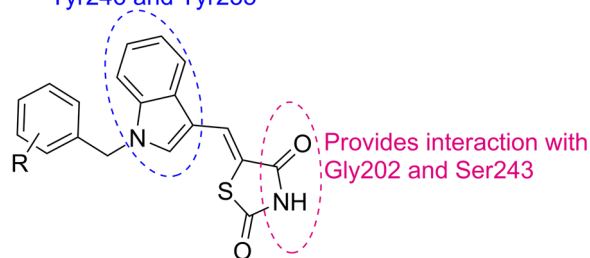


**Fig. 2** Pharmacophoric and interaction features required for the design of TZD-based PARP inhibitors

zamide group and an aromatic ring system [14]. In this context, thiazolidine-2,4-dione was chosen to provide the amide group required to form three hydrogen bond interactions with Gly202 and Ser243 amino acid residues. This TZD ring was condensed with an indole nucleus to provide a  $\pi - \pi$  stacking interaction with the aromatic amino acid Tyr246 (Fig. 2). Further, a benzyl ring with varied substituents was attached to the indole nitrogen and the impact of these substituents was assessed in *in vitro* assay results. The designed molecules were subjected to docking simulation using CDOCKER software in Discovery Studio (DS); the docking poses were first scrutinized for essential interactions and further optimized using the Prime MM-GBSA algorithm [15–18]. The CDOCKER binding energy and MM-GBSA scores of the synthesized molecules are listed in Table 1.

## Chemistry

Compounds **11–18** were synthesized using a two-step reaction process depicted in Scheme 1. In the first step, indole-3-carboxaldehyde was benzylated using substituted benzyl chlorides at the N-H position in the presence of the nucleophilic agent 1,8-diazabicyclo[5.4.0]undec-7-ene (DBU) in

DMF. The intermediates formed were purified by column chromatography using silica gel (100–200 mesh) and ethyl acetate and petroleum ether as solvent system. The presence of two singlets corresponding to the aliphatic benzyl proton ( $\sim 5$  ppm) and aldehyde proton ( $\sim 10$  ppm) in the  $^1\text{H-NMR}$  spectrum of the intermediates confirms the formation of the desired products. Intermediates **3–8** are reported in the literature [19–22], and their physicochemical properties (e.g., melting point) were found to be slightly different likely due to environmental fluctuations and manual errors. Subsequently, the substituted indole aldehydes were condensed via a Knoevenagel condensation reaction with thiazolidine-2,4-dione in the presence of  $\beta$ -alanine using acetic acid as solvent. The synthesis of the final compounds was confirmed by  $^1\text{H-NMR}$  based on the presence of a broad singlet at  $\sim 12$  ppm corresponding to the NH proton and a sharp singlet at  $\sim 5.5$  ppm corresponding to the aliphatic benzyl protons.  $^{13}\text{C}$  spectrum recorded two low-intensity signals at  $\sim 167$  ppm corresponding to two carbonyl groups and one signal at  $\sim 49$  ppm for the alkyl carbon. The benzyl chlorides considered for the reaction were substituted with different hydrophobic groups, including isopropyl, trifluoromethyl, methyl, chloro and fluoro.

## Biochemical activity

A PARP-1 enzyme assay indicates that compounds **12**, **13**, **15**, **16**, **17** and **18** have inhibitory activities comparable to 3-aminobenzamide (reference) (Table 1). Comparison of the docking results with the observed experimental PARP-1 inhibition showed that embedding hydrophobic groups (e.g., ethyl, isopropyl, *tert*-butyl) improved PARP inhibition. Substitutions at the R position of the TZD scaffold showed that ethyl, isopropyl, *tert*-butyl, trifluoromethyl and chloro groups improved inhibitory activity according to their respective lipophilic character. Moreover, the docked con-

**Table 1** Inhibitory activities of compounds **11–18** against PARP-1 enzyme

Compound	R	CDOCKER interaction energy	MM-GBSA score	IC <sub>50</sub> ( $\mu\text{M}$ )
11	H	−39.29	−67.48	>100
12	3-Cl	−43.67	−69.14	4.81 $\pm$ 2.31
13	4-F	−41.90	−66.48	5.03 $\pm$ 2.19
14	4-CH <sub>3</sub>	−43.77	−71.64	13.95 $\pm$ 6.59
15	3-CF <sub>3</sub>	−44.72	−72.07	3.07 $\pm$ 2.62
16	4-CH(CH <sub>3</sub> ) <sub>2</sub>	−47.04	−77.48	0.74 $\pm$ 0.25
17	4-(CH <sub>3</sub> ) <sub>3</sub>	−50.21	−87.62	0.82 $\pm$ 0.11
18	4-CH <sub>2</sub> CH <sub>3</sub>	−45.62	−79.86	1.56 $\pm$ 0.54
3-Aminobenzamide				4.78

IC<sub>50</sub> represents the dose of a compound in mole required to produce 50% inhibition of poly (ADP-ribose)polymerase enzyme. IC<sub>50</sub> values expressed as mean  $\pm$  SD,  $n = 2$ . MM-GBSA score shows the binding energy of the inhibitor to the protein expressed as kcal/mol

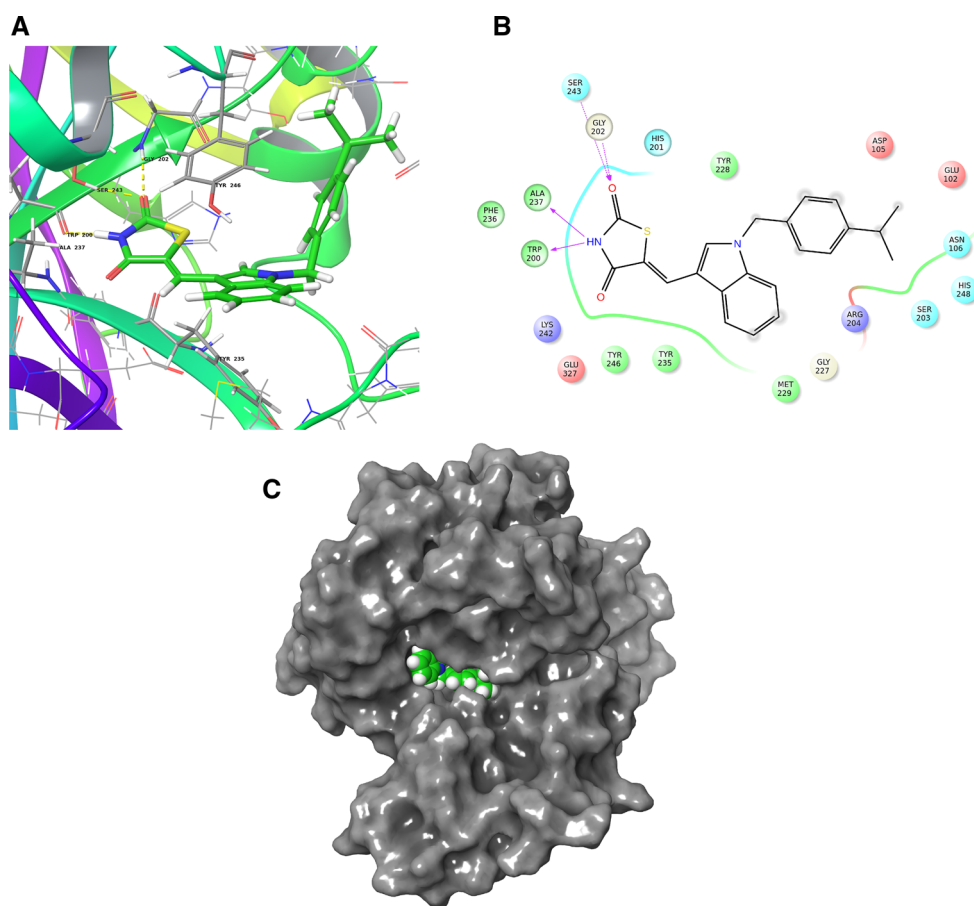


**Fig. 3** Docking interactions of hit compound **16** at the PARP-1 active site: **a** 3D view, **b** 2D view, **c** surface view

formations obtained for these structures confirmed that the larger groups could be accommodated well into the PARP-1 pocket. Docking of compound **16** ( $IC_{50} = 0.74 \pm 0.25 \mu\text{M}$ ) indicates that this analog fits well in the pocket (interactions shown in Fig. 3). However, while *tert*-butyl-containing compound **17** ( $IC_{50} = 0.82 \pm 0.11 \mu\text{M}$ ) exhibited similar inhibition to compound **16** ( $IC_{50} = 0.74 \pm 0.25 \mu\text{M}$ ), it did not improve PARP inhibition. This may be due to the steric clashes of the *tert*-butyl group within the active site of PARP-1. Thus, biochemical activity results show that a substitution of the hydrophobic group improves potency to submicromolar range and an isopropyl substituent is optimum for activity ( $IC_{50\text{value}} = 0.74 \mu\text{M}$ ).

## Conclusion

The investigation of the PARP-1 active site inspired us to design several new small thiazolidine-2,4-dione analogs for PARP inhibition using structure-based as well as knowledge-based approach. Compound **16**, with an isopropyl group, emerged as an attractive lead compound with an  $IC_{50}$  value of  $0.74 \pm 0.25 \mu\text{M}$ .

## Material and methods

### Chemistry

Chemicals and solvents utilized were of analytical grade or dry distilled. Reactions were monitored using thin-layer chromatography (TLC) with n-hexane/ethyl acetate (7:3) as mobile phase using pre-coated Merck silica gel aluminum sheets (Merck, India) and were visualized in an UV chamber. Synthesized compounds were purified using column chromatography using silica gel (mesh 100–200). Melting points were determined using open tubes in a paraffin bath and are uncorrected.  $^1\text{H-NMR}$  and  $^{13}\text{C-NMR}$  spectra were recorded on a Bruker AC 300 NMR Spectrometer (400 and 100 MHz, respectively), and chemical shift ( $\delta$ ) values were recorded as parts per million (ppm) using tetramethylsilane as internal standard. NMR abbreviations used are: singlet (*s*), doublet (*d*), triplet (*t*), quartet (*q*), quintet (quin.) and multiplet (*m*). Coupling constants are proved in Hertz (Hz). FTIR spectra were recorded on an FTIR Perkin-Elmer 1710 series as KBr pellets and signals recorded at  $\text{cm}^{-1}$  scale. Mass spectra were recorded on a Micromass Q-TOF spectrometer (Waters, MA, USA) in positive electrospray ionization (+ESI) mode. Melt-

ing points were determined using open tube method and the values were uncorrected.

### Synthesis of compounds 3–10

For the synthesis of intermediates 3–10, indole-3-carboxylaldehyde (5 mmol) was dissolved in appropriate quantity of dimethylformamide (DMF) followed by addition of 2.4 mL of 1,8-diazabicycloundec-7-ene and 6 mmol benzyl chloride. The mixture was refluxed for >20 h and the product was extracted by fractionation from ethyl acetate and water. The organic layer was concentrated to give crude product which was then purified using column chromatography (petroleum ether/ethyl acetate, 9:1). These compounds were characterized by <sup>1</sup>H NMR spectroscopy where the presence of a singlet at ~9 ppm confirms the presence of aldehyde group of indole while a sharp singlet appeared at ~5.5 ppm for CH<sub>2</sub> of benzyl group. The spectral data of compounds 3–10 are listed in Supplementary material.

### Synthesis of compounds 11–18

For the synthesis of final compounds, compounds 3–10 obtained from the previous step (0.3 mmol), β-alanine (6.0 mmol), thiazolidine-2,4-dione (6.0 mmol) and 10 mL glacial acetic acid were refluxed in a round-bottom flask for around 4 h. A small portion of water was added, the precipitate was collected by vacuum filtration, washed with glacial acetic acid, distilled water and ether. The solids were then dried at 40 °C. Further, the final compounds 11–18 were synthesized via Knoevenagel condensation in which the nucleophilic addition of the active methylene hydrogen of thiazolidine-2,4-dione to the carbonyl group of substituted indole-3-carbaldehyde is carried out in the presence of a catalytic amount of β-alanine. The most active compound 16 (5-((1-(4-isopropylbenzyl)-1H-indol-3-yl)methylene)thiazolidine-2,4-dione) was obtained as a yellow solid (81% yield) and a melting point in the range of 228–230 °C. The compound's IR spectrum showed the presence of band at ~ 3400 cm<sup>-1</sup> and strong absorption bands at ~ 1730 and ~ 1680 cm<sup>-1</sup> which were assigned to the two carbonyl groups. The <sup>1</sup>H NMR spectra of the compound showed that the isopropyl protons appear as a doublet at 1.17 ppm for (CH<sub>3</sub>)<sub>2</sub> and multiplet at 2.84 ppm for their adjacent CH proton. The aliphatic benzyl protons appear at 5.51 ppm, aromatic protons in the range of 7.18–8.18 ppm, while the thiazolidine-2,4-dione NH appears at 12.24 ppm. The <sup>13</sup>C NMR spectrum of compound 16 showed the presence of 22 carbons. The signals at 167.35 and 167.23 ppm correspond to the two carbonyl carbons of TZD ring, the aliphatic benzyl carbon appears at δ 47.87 ppm while the other aromatic carbons appeared at δ values of 110.27–147.98 ppm. The

mass spectrum of compound 16 showed quasi-molecular ion signal for [M+H]<sup>+</sup> at m/z 377.21 forming the base signal (100%). The spectral data of compounds 11–18 are listed in the Supplementary material.

### Biochemical activity

IC<sub>50</sub> values for PARP inhibition were determined by using a Trevigen HT Colorimetric PARP ELISA Assay kit (Cat# 4677-0960K). The assay was performed in 96-well histone-coated strip wells, according to the protocol provided by Trevigen. The strip wells were first rehydrated using the provided PARP buffer solution and incubated for 30 min. This was followed by adding a serial dilution of inhibitors, diluted PARP enzyme and a PARP cocktail (containing activated DNA, biotinylated NAD). The reaction was allowed to proceed for 60 min at room temperature. The strip wells were then washed with PBS and 0.1% Triton X-100 (2 times) and PBS (2 times). Thereafter, diluted streptavidin-linked peroxidase (Strep-HRP) was added to detect the extent of ribosylation and the mixture was incubated for 60 min. The plates were washed with PBS, followed by the addition of the TACS-Sapphire colorimetric substrate and allowed to develop color for 15 min in the dark. The reaction was stopped by adding 0.2N HCl, and the optical densities were read at 450 nm using an ELISA plate reader. All the data points were determined in triplicate, and the IC<sub>50</sub> value was obtained by plotting the % inhibition against log concentration values.

**Acknowledgements** Authors thank Council of Scientific and Industrial Research (CSIR), New Delhi, for providing funds for carrying out the research work (No. 02(0111)/12/EMR-II) and Department of Science and Technology (DST), New Delhi, for providing INSPIRE fellowship (No. IF150415). Authors also extend thanks to Sophisticated Analytical Instrumentation Facility, Punjab University, Chandigarh, for performing spectroscopic analysis and Apsara Innovations, Bengaluru, for extending technical support for performing *in silico* studies.

### Compliance with ethical standards

**Conflict of interest** Authors have no conflict of interests.

### References

- Rouleau M, Patel A, Hendzel MJ, Kaufmann SH, Poirier GG (2010) PARP inhibition: PARP1 and beyond. *Nat Rev Cancer* 10:293–301. doi:10.1038/nrc2812
- Rolli V, O'Farrell M, Ménissier-de Murcia J, de Murcia G (1997) Random mutagenesis of the poly (ADP-ribose) polymerase catalytic domain reveals amino acids involved in polymer branching. *Biochemistry* 36:12147–12154. doi:10.1021/bi971055p
- Javle M, Curtin NJ (2011) The role of PARP in DNA repair and its therapeutic exploitation. *Br J Cancer* 10:1114–1122. doi:10.1038/bjc.2011.382

4. Oliver FJ, Ménessier-de Murcia J, Nacci C, Decker P, Andriantsitohaina R, Muller S, de la Rubia G, Stoclet JC, de Murcia G (1999) Resistance to endotoxic shock as a consequence of defective NF- $\kappa$ B activation in poly (ADP-ribose) polymerase-1 deficient mice. *EMBO J* 18:4446–4454. doi:[10.1093/emboj/18.16.4446](https://doi.org/10.1093/emboj/18.16.4446)
5. Soriano FG, Virág L, Jagtap P, Szabó É, Mabley JG, Liaudet L, Marton A, Hoyt DG, Murthy KG, Salzman AL (2001) Diabetic endothelial dysfunction: the role of poly (ADP-ribose) polymerase activation. *J Mol Med* 7:108–113. doi:[10.1007/s001090100236](https://doi.org/10.1007/s001090100236)
6. Sodhi RK, Singh N, Jaggi AS (2010) Poly (ADP-ribose) polymerase-1 (PARP-1) and its therapeutic implications. *Vasc Pharmacol* 53:77–87. doi:[10.1016/j.vph.2010.06.003](https://doi.org/10.1016/j.vph.2010.06.003)
7. Canan Koch SS, Thoresen LH, Tikhe JG, Maegley KA, Almasy RJ, Li J, Yu X-H, Zook SE, Kumpf RA, Zhang C (2002) Novel tricyclic poly (ADP-ribose) polymerase-1 inhibitors with potent anticancer chemopotentiating activity: design, synthesis, and X-ray cocrystal structure. *J Med Chem* 45:4961–4974. doi:[10.1021/jm020259n](https://doi.org/10.1021/jm020259n)
8. Sandhu SK, Schelman WR, Wilding G, Moreno V, Baird RD, Miranda S, Hylands L, Riisnaes R, Forster M, Omlin A (2013) The poly (ADP-ribose) polymerase inhibitor niraparib (MK4827) in BRCA mutation carriers and patients with sporadic cancer: a phase 1 dose-escalation trial. *Lancet Oncol* 14:882–892. doi:[10.1016/S1470-2045\(13\)70240-7](https://doi.org/10.1016/S1470-2045(13)70240-7)
9. Roche H, Blum J, Eiermann W, Im Y-H, Martin M, Mina L, Rugo H, Visco F, Zhang C, Lokker N (2015) P1: 01 A phase 3 study of the oral PARP inhibitor talazoparib (BMN 673) in BRCA mutation subjects with advanced breast cancer (EMBRACA). *Ann Oncol* 26(supp-2):ii16. doi:[10.1093/annonc/mdv090.1](https://doi.org/10.1093/annonc/mdv090.1)
10. Tutt A, Robson M, Garber JE, Domchek SM, Audeh MW, Weitzel JN, Friedlander M, Arun B, Loman N, Schmutzler RK (2010) Oral poly (ADP-ribose) polymerase inhibitor olaparib in patients with BRCA1 or BRCA2 mutations and advanced breast cancer: a proof-of-concept trial. *Lancet* 376:235–244. doi:[10.1016/S0140-6736\(10\)60892-6](https://doi.org/10.1016/S0140-6736(10)60892-6)
11. Isakoff S, Overmoyer B, Tung N, Gelman R, Giranda V, Bernhard K, Habin K, Ellisen L, Winer E, Goss P (2011) A phase II trial of the PARP inhibitor veliparib (ABT888) and temozolomide for metastatic breast cancer. In: ASCO Annual Meeting Proceedings ed. 2010:1019 doi:[10.1158/0008-5472.SABCS11-P3-16-05](https://doi.org/10.1158/0008-5472.SABCS11-P3-16-05)
12. Plummer R, Lorigan P, Steven N, Scott L, Middleton MR, Wilson RH, Mulligan E, Curtin N, Wang D, Dewji R (2013) A phase II study of the potent PARP inhibitor, Rucaparib (PF-01367338, AG014699), with temozolomide in patients with metastatic melanoma demonstrating evidence of chemopotential. *Cancer Chemother Pharmacol* 71:1191–1199. doi:[10.1007/s00280-013-2113-1](https://doi.org/10.1007/s00280-013-2113-1)
13. Chadha N, Bahia MS, Kaur M, Silakari O (2015) Thiazolidine-2, 4-dione derivatives: programmed chemical weapons for key protein targets of various pathological conditions. *Bioorg Med Chem* 23:2953–2974. doi:[10.1016/j.bmc.2015.03.071](https://doi.org/10.1016/j.bmc.2015.03.071)
14. Chadha N, Silakari O (2016) Active site fingerprinting and pharmacophore screening strategies for the identification of dual inhibitors of protein kinase C  $\beta$  and poly (ADP-ribose) polymerase-1 (PARP-1). *Molec Divers* 20:747–761. doi:[10.1007/s11030-016-9676-9](https://doi.org/10.1007/s11030-016-9676-9)
15. Biovia Discovery Studio version 4.1, San Diego, CA, USA. <http://accelrys.com/>
16. Prime, Schrödinger, LLC, New York, NY, (2015). <https://www.schrodinger.com/prime>
17. Jacobson MP, Pincus DL, Rapp CS, Day TJF, Honig B, Shaw DE, Friesner RA (2004) A hierarchical approach to all-atom protein loop prediction. *Proteins* 55:351–367. doi:[10.1002/prot.10613](https://doi.org/10.1002/prot.10613)
18. Jacobson MP, Friesner RA, Xiang Z, Honig B (2002) On the role of crystal packing forces in determining protein sidechain conformations. *J Mol Biol* 320:597–608. doi:[10.1016/S0022-2836\(02\)00470-9](https://doi.org/10.1016/S0022-2836(02)00470-9)
19. Costi R, Cuzzucoli Crucitti G, Pescatori L, Messori A, Scipione L, Tortorella S, Amoroso A, Crespan E, Campiglia P, Maresca B (2013) New nucleotide-competitive non-nucleoside inhibitors of terminal deoxynucleotidyl transferase: discovery, characterization, and crystal structure in complex with the target. *J Med Chem* 56:7431–7441. doi:[10.1021/jm4010187](https://doi.org/10.1021/jm4010187)
20. Cavrini V, Gatti R, Roveri P, Cesaroni MR, Mazzoni A, Fiorentini C (1984) Syntheses and in vitro antimycotic activities of 1-benzyl-3-(1-imidazolylmethyl) indoles. *Arch Pharm* 317:662–668. doi:[10.1002/ardp.19843170803](https://doi.org/10.1002/ardp.19843170803)
21. Battaglia S, Boldrini E, Da Settimo F, Dondio G, La Motta C, Marini AM, Primofiore G (1999) Indole amide derivatives: synthesis, structure-activity relationships and molecular modelling studies of a new series of histamine H 1-receptor antagonists. *Eur J Med Chem* 34:93–105. doi:[10.1016/S0223-5234\(99\)80044-0](https://doi.org/10.1016/S0223-5234(99)80044-0)
22. Wu S, Wang L, Guo W, Liu X, Liu J, Wei X, Fang B (2011) Analogues and derivatives of oncrasin-1, a novel inhibitor of the C-terminal domain of RNA polymerase II and their antitumor activities. *J Med Chem* 54:2668–2679. doi:[10.1021/jm101417n](https://doi.org/10.1021/jm101417n)